JOURNAL OF OPTOELECTRONICS AND ADVANCED MATERIALS, Vol. 11, No. 1, January 2009, p. 62 - 69

Enhanced transition probabilities and trapping state emission of quencher impurities doped CaS:Mn phosphors

RAJESH SHARMA*, H. S. BHATTI[a], KWANGSEUK KYHM*
Research Center for Dielectric and Advanced Matter Physics, Department of Physics, Pusan National University, Busan 609-735, South-Korea
[a]*Department of Physics, Punjabi University, Patiala-147 002, India*

We have synthesized singly (Mn) and doubly doped (Mn and quencher impurities X = Fe, Co and Ni) CaS phosphor samples using high temperature synthesis technique. Photoluminescence (PL) excitation spectra of these phosphors show peak around 264 nm due to band to band/defect level excitation while emission spectra show strong 585 nm emission peak which is due to incorporation of Mn impurity in host CaS phosphor. Adding the quencher impurities to CaS:Mn phosphors, no considerable change was observed in the emission spectra. The weak luminescence due to quencher impurities in CaS phosphors was suppressed by strong and broad band orange emission of Mn impurity, as the samples were doubly doped with Mn and quencher impurities. Enhancement of photoluminescence intensity of CaS:Mn:Co phosphors was reported in comparison to CaS:Mn:Ni or Fe phosphors at liquid nitrogen temperature. Although we observed no appreciable change in PL spectra of CaS:Mn phosphors co-doped with quencher impurities, ten-fold increase in the transition probabilities was noticed. A dynamic charge carrier relaxation model has been proposed to explain the observed abnormal behaviour of shallow and deep trap state emission from CaS:Mn, X doped phosphors.

(Received July 5, 2008; accepted January 21, 2009)

Keywords: Trap-depth values, Quencher impurities, CaS:Mn phosphors, Radiative transition probabilities, Laser induced excitation

1. Introduction

The use of intentional impurities, or dopants, to control the behavior of materials lies at the heart of many technologies [1-8]. Doping is critical for phosphors, which would otherwise be electrically insulating. For this reason, researchers have begun to explore how dopants can influence optical and electronic behavior of host phosphors. Undoped phosphors can now be prepared from most common group IV, III-V, and II-VI semiconductors, as well as in different shapes such as nanorods, tetrapods, and nanowires [9-12]. They can be easily manipulated as colloidal dispersions and used as building blocks to create a family of complex artificial solids. The promise of phosphors, as a technological material, for applications including wavelength tunable lasers, bioimaging, and solar cells, may ultimately depend on tailoring their behavior through specific doping. Impurities can strongly modify electronic, optical, and magnetic properties of bulk phosphor material [13-20]. Although undoped phosphors are weakly fluorescent with a colour that depends on size, laser fabrications based on this emission are intrinsically inefficient. Several approaches can improve this situation, and one possibility is to incorporate dopants that provide carriers [21-25]. The energy from absorbed photons can be efficiently transferred to the impurity, quickly localizing the excitation and suppressing undesirable effects on the phosphor surface. For magnetic dopants, addition of the impurity within the host material can enhance its interactions with other carriers or quantum mechanical spins.

In fact, Mn and Fe or Co or Ni provides excellent systems to study doping because they have unique magnetic and optical properties [4, 5, 8, 10]. However, in II-VI phosphors, they are isovalent with the atoms for which they substitute and hence cannot provide extra electrons or holes. Attempts at heterovalent doping have begun only recently, including Mn-doped InAs and Li doped ZnO, as well as P- and B-doped Si grown in the solid phase [9]. Despite doping successes, puzzles have also arisen. The actual amount of impurity incorporated at host lattice sites is typically less than the concentration of impurity added during synthesis [26-28]. For Mn, in II-VI phosphors, which has high bulk solubility (tens of percent), the concentrations attained in nanocrystals are far smaller (1% or less) [7, 10]. Indeed, early efforts to dope Mn into other host lattices failed to incorporate any impurities. These unexplained results have led to theoretical efforts to understand the mechanisms that control doping. Lehmann [4] had reported the synthesis of CaS phosphors by individually doping 31 different activator ions. He reported that the luminescence from Fe, Co and Ni ions was quenched when added to the CaS

lattice. To improve the longevity of phosphor-converted white light-emitting diode (LED), CaS:Eu red phosphor is usually coated by SiO_2 [29]. The coating characteristics such as moisture resistance were found to be excellent and critically dependent upon the processing variables such as precursor concentration, pH value, and the temperature of the solution in case of the sol–gel process. In another report, He et al. [30] prepared CaS:Eu red-emitting phosphor particles using precipitation method, followed by sintering in the atmosphere over the mixture of sulfur powder, Na_2CO_3, and carbon-containing compounds such as tartaric acid, citric avid, glucose, and cane sugar. The structure, morphology and photoluminescence performance of the phosphor samples were investigated in detail using x-ray powder diffraction (XRD), transmission electron microscopy (TEM), and photoluminescence spectrum (PL), respectively [31-35]. CaS:Eu^{2+} particles without additive show inhomogeneous, rough and aggregation with the size of 75–125 nm, but the spherical particles with mean size of about 110 nm were obtained by adding carbon-containing compounds. Recently, we have reported a successful doping of Co and Fe impurities in ZnS:Mn nanophosphors and also studied their photoluminescence [10, 13]. The PL spectra of ZnS:Mn, Co show three peaks at 410, 432 and 594 nm while location of the peaks was altered in case of ZnS:Mn, Fe nanophosphors. The success of this work at nanoscale domain motivated us to study the carrier relaxation in CaS:Mn phosphors doped with quencher impurities at bulk scale which was almost vague in the literature. Two systems are quite different as in case of ZnS nanoparticles the quantum confinement effect dominates, and the optical properties are modified due to higher surface to volume ratio. The bulk band gap is different i.e. ~3.7eV for ZnS and ~4.7eV for CaS phosphors. Consequently the phosphor chemistry of these two materials is quite different and interesting aspect. Moreover the traps are introduced at different trap-depths in these two host materials.

Although in recent years large number of research papers [6-9, 10, 11, 14-16, 28-30] reporting useful industrial applications of doped CaS phosphors were published, the details of the trapping states introduced by quencher impurities [4, 8, 13, 23, 24] is still vague and interesting aspect. In this paper, we report the doping of CaS phosphors using high temperature synthesis technique with Mn, and Mn as well as quencher impurites. The PL energy resolved spectra studies were carried out at room temperature. The transition probabilities, trap-depth and decay constant values at 77 K temperature were calculated exciting these phosphors using a pulsed UV N_2 laser. The observed optical properties were explained using carrier relaxation and recombination model.

2. Experimental arrangements

CaS doped phosphors with variable concentration of dopants were synthesized in the laboratory whose details are already reported in our previous publication [8]. Four series of samples (A - D) with different permutation of dopant concentration were prepared which are listed in Table 1.

Photoluminescent (PL) energy resolved spectra at room temperature were recorded using spectrofluorometer, JASCO-FP- 6500, fitted with a 350 W Xenon flash lamp and R-928 photomultiplier tube (PMT) detector. The detail of the experimental set-up for recording luminescence decay curves were already reported in our recent publication [13]. Briefly, the sample was pasted on to the cold copper finger of cryostat for transition probability measurement at 77 K. The required vacuum was created using a cryostat and then flow of liquid nitrogen was made. The 77 K temperature was obtained in the cryostat using temperature sensitizer. Nitrogen laser [8, 10, 13] is a suitable excitation source (pulse width ~ 10 ns and output peak power ~ 200 kW) for photoluminescence decay measurements whose high photon flux density was extremely useful to excite the short-lived shallow trapping states. The fluorescence/phosphorescence emission was collected at an angle of 90° to the incident beam using a fast photomultiplier tube (PMT). Then the emitted visible radiation was allowed to pass through an assembly of monochromator and glass slab which was used as a UV filter. The photoluminescence decay signals from the phosphors were recorded by digital storage oscilloscope coupled to computer assembly. These decay curves were analysed by computer simulations to obtain two or three transition probability values.

3. Results and discussion

3.1 PL studies

Fig. 1 shows the PL spectra of CaS:Mn doped phosphors at room temperature. In the figure, the curve A represents the excitation spectra of CaS: Mn doped phosphor sample which shows its peak around 264 nm. As, the bulk band gap of CaS phosphor is ~ 4.7eV [4] hence it comes under the category of a wide band gap phosphor material. However, the defects of polycrystalline solids always play an important role in emission spectra of phosphor material.

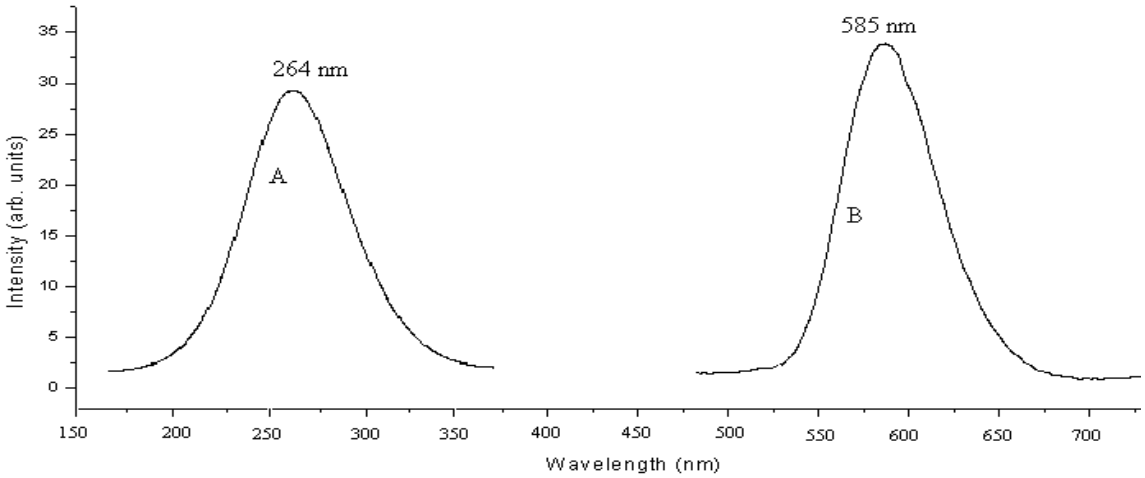

Fig. 1. Photoluminescence excitation and emission spectra for CaS :Mn phosphor at room temperature.

Consequently, we ignore the possibility of band-edge emission in these phosphors but this peak might be originated due to some transition from defect level introduced below the conduction band and above the valence band of host CaS. Hence, the peak is assigned due to the transition between two defect levels and may be very near to band to band excitation. On the other hand, the curve B represents the emission spectra of CaS doped phosphor with peak around 585 nm, however, the tail of this curve extends to 750 nm region. The peak around 585nm was also reported in ZnS:Mn bulk and nanophosphors [1,6 7, 10]. The emission centered around 585 or 590 nm was reported by many researchers [1, 10, 13, 14] when Mn is incorporated in sulphide phosphors. So, this peak may be due to Mn impurity related emission. The levels introduced by Mn impurity in sulphide phosphor are $^4T_1$-$^6A_1$. This transition is forbidden by spin selection rules and the probability of this transition is very low. Also, we observed almost no change in the emission spectra when CaS:Mn phosphors were co-doped with the quencher impurities. Although, it was reported in the literature that Fe and Ni show blue-green and orange-red emissions respectively, in CaS doped phosphor material [4]. Also Co shows its emission peak around 450 nm when incorporated in CaS lattice [15]. Recently, Sapra *et al.* [12] reported that the defect related emission around 425 nm for ZnS:Mn nanophosphor was suppressed by the presence of strong emission of Mn impurity. They had shown that on increasing the concentration of Mn in the host material, the defect related emission is completely quenched due to strong and broad band emission of Mn impurity. Although, the two phosphors are quite different in terms of introduction of trap states in host band gap but the quenching of weak emission in comparison to strong one is a most common fact observed in the phosphors. Hence, we believe that almost similar quenching of the emission might have occurred from quencher doped CaS:Mn phosphor in the present case. The emission spectrum of Mn doped sample in the present studies is entirely dominated by orange Mn emission which may be the cause of absence of Fe or Co or Ni emission.

3.2 Transition probability, trap-depth and decay constant studies

The luminescence decay curves obtained from time resolved photoluminescence (TRPL) studies were analyzed to deduce the transition probability values. Ln intensity vs time graph were plotted for each decay curve of Fig. 2 using computer software which were further peeled off [8, 10, 13] into two or three components. The slope of these components produced three probability values (p_1, p_2 and p_3). The largest (p_1) of the three calculated probabilities is due to the transitions in the trapping levels close (shallow) to the conduction band while the least probability value (p_3) is tentatively attributed to the decay from the deeper levels.

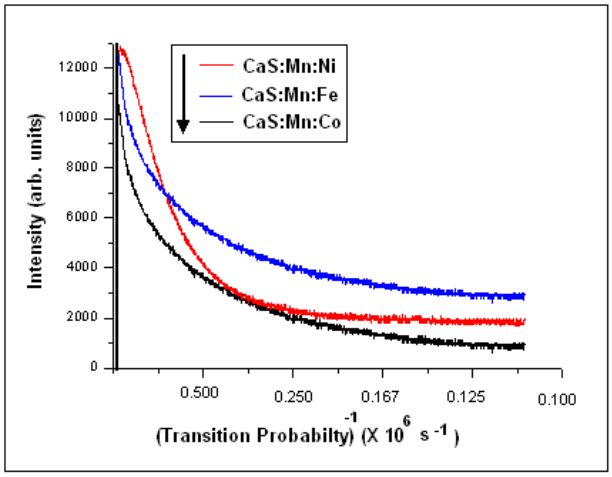

Fig. 2 Multi-exponential photoluminescence decay curves of CaS:Mn phosphors co-doped with Fe or Co or Ni at liquid nitrogen temperature. The downward arrow indicates the sequence (starting from top to bottom) of luminescence decay curves for CaS:Mn:Ni, CaS:Mn:Fe and CaS:Mn:Co phosphors (see text for more details)

The intermediate probability value (p_2) is due to the transitions between the levels which are in between the

two trapping state levels. This means that there are multiple trapping levels at different depths below the conduction band or above the valence band, which were introduced by dopants in the host material. From the slope of line, which provide the value of 'p', one can calculate value of trap-depth, E, according to the Boltzmann's equation. The details of calculations of trap-depth values are reported elsewhere [8, 10].

Figure 2 shows comparison of luminescence decay curves for CaS:Mn:Ni, CaS:Mn:Fe and CaS:Mn:Co phosphors at 77 K temperature. The transition probability values were found to be $3.57X10^6$, $0.64X10^6$ and $0.18X10^6$ s^{-1} for CaS:Mn:Ni phosphor while in case of CaS:Mn:Fe phosphor these values reduce to be $0.52X10^6$, $0.35X10^6$ and $0.08X10^6$ s^{-1}. Also, the transition probability values were found to be $0.58X10^6$, $0.30X10^6$ and $0.05X10^6$ s^{-1} for CaS:Mn:Co phosphor. Basically, three probability values were found for each sample so there are identical numbers of trapping levels introduced by the dopants contributing to the radiative transitions. Owing to the addition of Fe to CaS :Mn phosphor, the contribution of the non-radiative transition was quenched by Fe impurity and enhanced radiative emission intensities are observed in present investigation. Table 1 shows the variation of the trap-depth and decay constant values of CaS:Mn and CaS: Mn, X at 77 K temperature. Figure 3 shows the variation of trap-depth values with dopant concentration of CaS doped phosphors at 77 K temperature. In Fig. 3(a), the concentration of the Mn impurity in host CaS was varied from 0.05 to 0.70%. E_1, E_2 and E_3 are the trap-depth values of shallow, intermediate and deep trapping levels, respectively. Here, $A:E_1$ shows the variation of shallow trapping states which contribute to radiative transition for different concentration (0.05, 0.30 and 0.7 %) of Mn^{2+} ions in host CaS phosphor. In this case the corresponding trap-depth values decrease with the increase in concentration of Mn in host CaS phosphor which shows that there is a probability that the electron may be captured by defect level for small concentration of Mn and then the energy may be transferred from defect level to Mn centre. On still increasing Mn concentration there is a considerable delay in the radiative emission which leads to smaller radiative transition probability values. With increased concentration of Mn in host CaS, band to band excitation energy might be directly transferred to Mn impurity centres. Consequently, the probability of the $^4T_1$-$^6A_1$ transition of Mn centres increase which reduce the radiative trap-depth values.

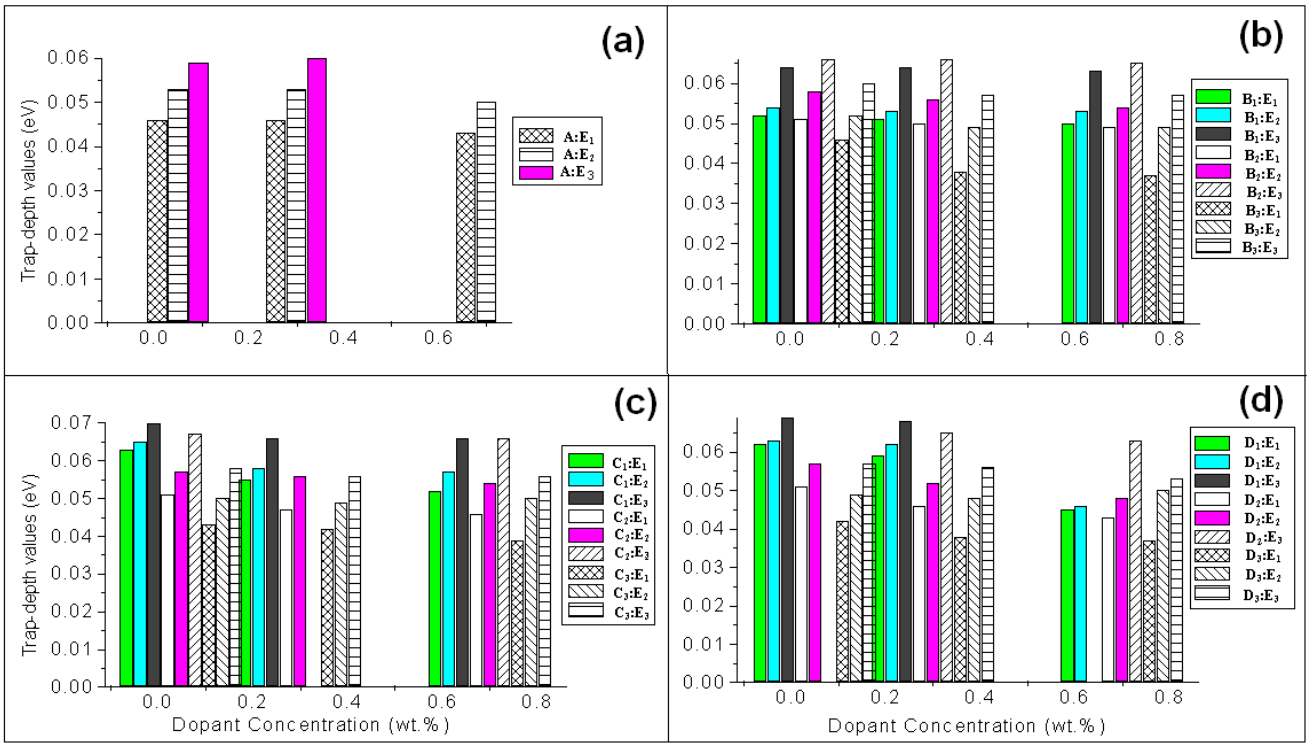

Fig. 3 Schematic variation of trapping state values with dopant concentration in CaS doped phosphors at liquid nitrogen temperature: (a) singly doped with variable concentration of Mn impurity from 0.05-0.70 %, (b) the concentration of Mn was kept constant at 0.05 % while quencher impurity concentration varied from 0.05-0.70 %, (c) the concentration of Mn was kept constant at 0.30% while quencher impurity concentration varied from 0.05-0.70 %, (d) the concentration of Mn was kept constant at 0.70% while quencher impurity concentration varied from 0.05-0.70 % (see text and Table 1 for comparison of concentration of dopants).

As the decay curve for CaS:Mn (0.70%) phosphor sample was found to be overlapping of two exponentials (see Table 1 for details) so only two values of trap-depths were deduced (0.043 and 0.050 eV). In case of CaS:Mn phosphors, the trap-depths vary from 0.043-0.060 eV.

Fig. 3(b) shows the variation of the trap-depth values of doubly doped samples. Here concentration of Mn was kept constant at 0.05% while that of quenchers were varied from 0.05-0.70%. In sample series B_1, B_2 and B_3, the Mn concentration was fixed at 0.05% while other dopants were Fe (0.05, 0.30 and 0.70%), Co (0.05, 0.30 and 0.70%) and Ni (0.05, 0.30 and 0.70%), respectively. For B series, the trap-depth value was found to be maximum i.e. 0.066 eV for CaS: Mn (0.05%), Co (0.05%) and CaS:Mn (0.05 %), Co (0.30 %) doped phosphors while it was minimum i.e. 0.037 eV for CaS:Mn (0.05%), Ni (0.70%). Fig. 3(c) shows the variation of the trap-depths for the sample series C with fixed Mn(0.30%) concentration while that of quenchers varied from 0.05-0.70%. Here the trap-depth value was maximum i.e. 0.070 eV for CaS: Mn (0.30%), Fe (0.05%) doped phosphor while minimum i.e. 0.039 eV for CaS:Mn (0.30%), Ni (0.70%). The sub-panel (d) of Figure 3 shows the variation of the trap-depths for the sample (series D). In the sub-panel, Mn concentration was fixed at 0.70 % and the quencher concentration varied from 0.05-0.70%. In this case, the trap-depth was found to be maximum i.e. 0.069eV for CaS: Mn (0.70%), Fe (0.05%) doped phosphor while minimum value i.e. 0.037 eV was obtained for CaS:Mn (0.70%), Ni (0.70%). For this sample, the value of the transition probability was found to be 3.7×10^6 s^{-1} which shows 10 fold increase in comparison to CaS:Mn phosphors i.e. 14.9×10^5 s^{-1}.

Table 1. Schematic representation of trap-depth and decay constant values for CaS:Mn and CaS:Mn, X phosphors

Phosphor Sample Series	**Phosphor: Impurity (wt. %)**	**Trap Depths (eV) at 77 K**			**Decay Constant**
		E_1	**E_2**	**E_3**	b
A	CaS:Mn (0.05)	0.046	0.053	0.059	0.67
	CaS:Mn (0.30)	0.046	0.053	0.060	1.31
	CaS:Mn (0.70)	0.043	0.050	--	1.77
B_1	CaS:Mn(0.05):Fe(0.05)	0.052	0.054	0.064	0.65
	CaS:Mn(0.05):Fe(0.30)	0.051	0.053	0.064	0.89
	CaS:Mn(0.05):Fe(0.70)	0.050	0.053	0.063	0.88
B_2	CaS:Mn(0.05):Co(0.05)	0.051	0.058	0.066	0.67
	CaS:Mn(0.05):Co(0.30)	0.050	0.056	0.066	1.45
	CaS:Mn(0.05):Co(0.70)	0.049	0.054	0.065	1.44
B_3	CaS:Mn(0.05):Ni(0.05)	0.046	0.052	0.060	1.32
	CaS:Mn(0.05):Ni(0.30)	0.038	0.049	0.057	1.22
	CaS:Mn(0.05):Ni(0.70)	0.037	0.049	0.057	1.56
C_1	CaS:Mn(0.30):Fe(0.05)	0.063	0.065	0.070	0.85
	CaS:Mn(0.30):Fe(0.30)	0.055	0.058	0.066	0.78
	CaS:Mn(0.30):Fe(0.70)	0.052	0.057	0.066	0.69
C_2	CaS:Mn(0.30):Co(0.05)	0.051	0.057	0.067	0.77
	CaS:Mn(0.30):Co(0.30)	0.047	0.056	---	1.09
	CaS:Mn(0.30):Co(0.70)	0.046	0.054	0.066	1.19
C_3	CaS:Mn(0.30):Ni(0.05)	0.043	0.050	0.058	1.45
	CaS:Mn(0.30):Ni(0.30)	0.042	0.049	0.056	0.78
	CaS:Mn(0.30):Ni(0.70)	0.039	0.050	0.056	0.84
D_1	CaS:Mn(0.70):Fe(0.05)	0.062	0.063	0.069	0.77
	CaS:Mn(0.70):Fe(0.30)	0.059	0.062	0.068	0.71
	CaS:Mn(0.70):Fe(0.70)	0.045	0.046	---	0.65
D_2	CaS:Mn(0.70):Co(0.05)	0.051	0.057	---	1.18
	CaS:Mn(0.70):Co(0.30)	0.046	0.052	0.065	1.16
	CaS:Mn(0.70):Co(0.70)	0.043	0.048	0.063	0.91
D_3	CaS:Mn(0.70):Ni(0.05)	0.042	0.049	0.057	0.76
	CaS:Mn(0.70):Ni(0.30)	0.038	0.048	0.056	0.75
	CaS:Mn(0.70):Ni(0.70)	0.037	0.050	0.053	0.72

The trap-depth values increased with the addition of Fe and Co dopants to CaS:Mn phosphor which shows that these impurities introduce shallow trapping levels in the energy band gap of host phosphor. Also the trap-depth values decrease to 0.037 eV on addition of Ni impurity to CaS:Mn doped phosphors so the levels responsible for radiative transitions are lying relatively deeper in the forbidden gap of CaS. We believe that the electrons trapped in the deeper energy levels might be unable to make a transition to the conduction band due to lack of sufficient energy which results in faster energy transfer from the Ni to Mn centres. The faster energy transfer

increases the radiative transition probability and thus radiative trap-depth values were reduced. But, in case of the co-doping with Fe and Co, the electrons trapped in the shallow energy levels are thermally excited to the conduction band and the energy is transferred to $^4T_1$-$^6A_1$ energy levels.

The distribution of the traps in energy band gap of doped phosphor can be studied from decay constant, b, variation of different samples [8, 10, 13]. The value of decay constant carries the information about the distribution of the dopant trapping states introduced within the band gap of the phosphor. If the value of decay constant is unity [11,13], the impurity traps are uniformly distributed in the band gap of the phosphor, otherwise, there may be non-uniform distribution of the traps. Fig. 4 shows the variation of the decay constant values for series A, B, C and D at 77 K temperature. The decay constant values show that the trapping states which contribute to the radiative transitions are non-uniformly distributed in energy band gap of the present host material. Unlike trap-depth values, we could not find any schematic variation of decay constant with the increase/decrease of the dopant concentration. For series, C_1, D_1 and D_3, the decay constant values were almost identical while for the other series sharp variation was noticed with increasing concentration of dopant ions. As the samples of series C_1, D_1 were containing higher concentration (0.3 and 0.7%) of Mn impurity there may be perturbation of the Mn levels due to addition of the quencher impurities to CaS:Mn phosphors which may perhaps resulted in large variation of the decay constant values [11, 13]. The excitation of shallow traps of phosphors under investigation were mainly attributed to high peak power output and short pulse-width of the exciting nitrogen laser source, otherwise, trap-depth values obtained using ordinary excitation sources were relatively large in comparison to present study.

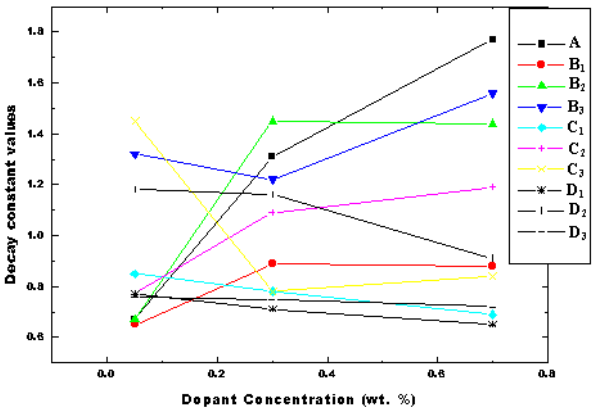

Fig. 4. Decay constant variation with dopant concentration for CaS:Mn and CaS:Mn, X phosphors at liquid nitrogen temperature.

The non-availability of high peak power output and short pulse-width of the ultraviolet source was probably the reason why the earlier workers [4] could not get the luminescence from shallow trapping states in the case of these quencher impurities. Further there are number of aspects which may be responsible for observed behavior of transition probabilities, trap-depths and decay constant variation of CaS:Mn,X phosphors. The observed cause for this variation is described below in details.

In almost all of these systems of CaS phosphors, the dynamics of photogenerated charge carriers appear to be dominated by trapping and subsequent recombination of trapped carriers caused by surface trap states. Figure 5 shows schematically the major pathways for charge carrier relaxation following above band gap photoexcitation. The first step of relaxation should be electronic relaxation in the conduction band and hole relaxation in the valence band.

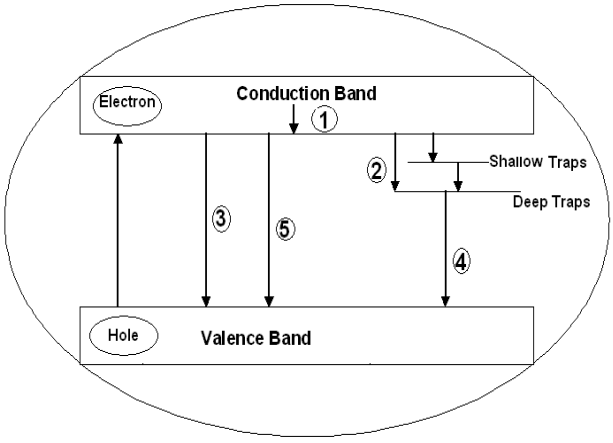

Fig.5 Schematic illustration of charge carrier relaxation in CaS phosphors. The line with upward arrow indicates excitation while downward arrow indicate different relaxation processes; (1) electronic relaxation within the conduction band, (2) trapping into shallow trap (ST) and deep trap (DT) states and further trapping from ST to DP, (3) bandedge electron-hole recombination, (4) trapped electron-hole recombination, and (5) exciton-exciton annihilation.

This is mainly due to electron-phonon interaction and is expected to be on the time scale of 100 fs or less. Once the electron is relaxed to the bottom of the conduction band and the hole to the top of the valence band, they can recombine radiatively or nonradiatively. If there are few or no band gap states, the recombination should be primarily radiative, i.e., strong bandedge luminescence should be observed, and the lifetime should be on the order of nanoseconds or longer. This bandedge emission was not obtained in our measurements due to presence of impurities in host material. When states are present within the band gap due to surface or internal defects, they act to trap the charge carriers on time scales faster than radiative recombination, typically a few picoseconds to tens of picoseconds. Further trapping from shallow trap states to deep trap states can take place on the tens of ps to hundreds of ps time scales. The trapped charge carriers can recombine nonradiatively or radiatively, producing trap state emission that is red shifted with respect to bandedge

emission. The trap states have lifetimes on the time scale from tens of picoseconds to nanoseconds or microsecond or even longer, depending on the nature of the trap states. We believe that the transition probability, trap-depth and decay constant values deduced in present investigations are due to trap state emission in CaS doped phosphors. The trap states also vary significantly in their energy levels or trap depth, which in turn determines how fast the trapping occurs and how long the trap states live. It should also be pointed out that the excitonic state, formed as a result of coulombic interaction between the electron and hole, usually lies slightly below the bottom of the conduction band (few tens of meV) but above the trap states. This excitonic state can also be populated during the relaxation process. However, since the binding energy of the exciton is typically small, it is generally difficult to experimentally distinguish between the bottom of the conduction band and the excitonic state. We will simply refer to them as band-edge states in our measurements.

4. Conclusions

In summary, we demonstrated that the decreasing trend of the trap-depth values with increasing concentration of Mn in case of CaS:Mn phosphors is attributed to the fact that the emission from shallow trapping states plays a significant role. As quencher impurities (Fe or Co) are added to CaS:Mn phosphors, the trap-depth values increase showing the emission from shallow trapping states. These relatively shallow trapping states introduced in the band gap of the host material are due to the Fe or Co impurities added to the CaS:Mn phosphors. But in case of CaS:Mn doped with Ni trap-depth values decrease due to the reason that there is a faster energy transfer from Ni to Mn level. The radiative transition probabilities were observed to increase by ten-fold on addition of killer impurity (Ni) to CaS:Mn phosphor which strongly suggests that doping has enhanced the properties of phosphors by providing another means to control their remarkable electronic and optical properties. In this sense, the development of doped phosphor materials is mirroring the evolution of bulk semiconductors half a century ago. Future progress in doped phosphors will require improving synthetic control over dopant incorporation, optimizing their concentrations, and investigating the phenomena that emerge. Pursuing these goals, and enhanced optoelectronic applications would be an exciting and challenging task for the future research.

Acknowledgements

This work was supported by the Korean Research Foundation Grant funded by the Korean Government (MOEHRD) (KRF-2007-313--C00219) and Korean Research Foundation Grant (KRF-2006-005-J02802).

References

[1] K.Manzoor, V. Aditya, , S. R. Vadera, N. Kumar, T. R. N. Kutty, Solid State Commun. **135**, 16 (2005).
[2] B. Gilbert, H. Huang, H. Zhang, G. A. Waychunas, J. F. Banfield, Science 305 651, (2004).
[3] S. Coe, W. K.Woo, M. G. Bhawendi, V. Bulovic, Nature **370**, 354 (2003).
[4] W. Lehmann, J. Lumin. 5, 87 (1972).
[5] H. Choi, C. H. Kim, C. H. Pyun, S. J. Kim, J. Lumin. **82**, 25 (1999).
[6] D. Jia, J. Zhu, B. Wu, J. Lumin. **90**, 33(2000).
[7] A. Cho, S. Y. Kim, M. Lee, S. J. Kim, C. H. Kim, C. H. Pyun, J. Lumin. **91**, 215(2000).
[8] H. S. Bhatti, Rajesh Sharma, N. K. Verma, Physica B: Physics of Condensed Matter, **382**, 38 (2006).
[9] J.D. Bryan and D.R. Gamelin, Prog. Inorg. Chem. **54**, 47, (2005).
[10] H. S. Bhatti, Rajesh Sharma, N. K. Verma, N. Kumar, S. R. Vadera and K. Manzoor, J Phys. D: Appl. Phys., **39**, 1754 (2006).
[11] P.I. Paulose, James Joseph, M.K. Rudra Warrier, Gijo Jose, N.V. Unnikrishnan, J. Lumin. **127**, 583 (2007).
[12] S. Sapra, A. Prakash, A. Ghangrekar, N. Periasamy, D. D. Sharma, J. Phys. Chem. B **109**, 1963 (2005).
[13] Rajesh Sharma and H. S. Bhatti, Nanotechnology, **18**, 465703 (2007).
[14] Ping Yang, Meng Kai Lü, Chun Feng Song, Dong Xu, Duo Long Yuan, Feng Gu Mater. Chem. Phys. **91**, 253 (2005).
[15] Vijay Singh, T.K. Gundu Rao, Jun-Jie Zhua, Manoj Tiwari Mater. Sci. Engg. B **131**, 195 (2006)
[16] Dongdong Jia a, Xiao-jun Wang, Opt. Mater. **30**, 375(2007).
[17] P. Smet, J. V. Gheluwe, D. Poelmann, R. L. V. Meirhaeghe, J. Lumin. **104**, 145 (2003).
[18] P. Smet, D. Wauters, D. Poelmann, R. L. V. Meirhaeghe, Solid State Commun. **118**, 59 (2001).
[19] T. V. Samulski, P. T. Chopping, B. Haas, Phys. Med. Biol. **27**, 107 **(**1982).
[20] R. N. Bhargava, D. Gallagher, X. Hong, A. Nurmikko, Phys. Rev. Lett. **72**, 416 (1994).
[21] R. N. Bhargava, J. Lumin. **70**, 85 (1996).
[22] N. Murase, R. Jaganathan, Y. Kanemastu, M. Watanabe, A. Kurita, K. Hirata, T. Yazama, T. Kushida, J. Phys. Chem. B **103**, 754 (1999).
[23] P. Yang, M. Lu, D. Xu, D. Yuan, C. Song, G. Zhou, J. Phys. Chem. Solids **62**, 1181(2001).
[24] P. Yang, M. Lu, D. Xu, D. Yuan and G. Zhou, Chem. Phys. Lett. **336**, 76 (2000).
[25] H. Choi, C. H. Kim, C. H. Pyun and S. J. Kim, J. Solid State Chem. **138**, 149 (1998).
[26] C. R. Ronda, J. Lumin.; **72-**74, 49 (1997).
[27] D. Wauters, D. Poelmann, R. L. V. Meirhaeghe, J. Phys.: Conden. Matter 12, 3901 **(**2000).
[28] P. J. Liu, Y. L. Liu, Chinese Chem. Lett. **11**, 843 (2000).

[29] Hyun Ho Shin, Jin Hyung Kim, Bo Yong Han, and Jae Soo Yoo, Jpn. J. Appl. Phys.,**47**, 3524 (2008).
[30] Xiang-Hong He and Ying Zhu, J. Mater. Sci. **43**, 1515 (2008).
[31] A. Cho, S. Y. Kim, M. Lee, S. J. Kim, C. H. Kim, C. H. Pyun, J. Lumin. **91**, 215 (2000).
[32] H. Nanto, M. Ikeda, M. Kadota, J. Nishishita, S. Nasu, Y. Douguchi, Nucl. Instrum. Meth. B **116**, 262 **(**1996).
[33] Yoshiyuki Kojima, Kenichi Aoyagi, Tamotsu Yasue J. Lumin. **126**, 319 (2007).
[34] Shreyas S. Pitale, Suchinder K. Sharma, R.N. Dubey, M.S. Qureshi, M.M. Malik, Nucl. Instr. and Meth. in Phys. Res. B 266, 2027 (2008).
[35] Chongfeng Guo, Dexiu Huanga, Qiang Su Mater. Sci. Engg. B **130**, 189 (2006).

*Corresponding author: sharma_rajesh1234@yahoo.com
kskyhm@pusan.ac.kr